

Chapter 2

Experimental Setup

The 14 UD Bhabha Atomic Research Center-Tata Institute of Fundamental Research (BARC-TIFR) accelerator facility was utilized to perform the present experimental work. The 16 MeV of proton beam was utilized for the proton irradiation and the neutrons were generated for different energies using ${}^7\text{Li}(\text{p}, \text{n})$ reaction. The activation method and offline gamma ray spectroscopy were adopted to carry out the irradiation experiment. This chapter contains the detail of the experiment, accelerator facility, and detector set-up.

2.1 Introduction

Accelerators were designed to generate energetic particles for investigating the nuclear structure and other aspects of nuclear physics. The machine is utilized to increase the speed (accelerate) of the charged particles using the electric field and the magnetic field which is used to focus steer and generate a well-defined beam. The accelerators are of two types, (i) Electrostatic accelerators (e.g. Van de Graff Generator, Cockcroft-Walton), and (ii) Oscillating fields (e.g. Linacs, cyclotron, synchrotron). The electrostatic accelerators use the static electric field for particle acceleration that requires a large electric field to achieve experimentally required energy. Therefore, the second type of accelerator was developed which uses an electric field changing with time. This changing electric field can accelerate particles to very high energies, leading to many key discoveries [1]. In the present study, the LINAC pelletron accelerator was used to experiment. A brief idea of the accelerator is given in the section below.

2.2 BARC-TIFR Accelerator

The experimental facility provided by the Tata Institute of Fundamental Research is the combined project of the Bhabha Atomic Research Center and Tata Institute of Fundamental Research (BARC-TIFR) [2].

The experimental facility provided by the Tata Institute of Fundamental Research is the combined project of the Bhabha Atomic Research Center and Tata Institute of Fundamental Research (BARC-TIFR) [2]. The 14-UD Medium Energy Heavy-Ion Accelerator (MEHIA) is extensively utilized for fundamental research in nuclear, condensed matter, atomic, and multidisciplinary areas [3]. It is an electrostatic accelerator working as a charge exchange system. It consists of a chain of small metal pellets detached via nylon links that carry out charges towards the terminal for increasing its potential to 14 MV [4] and hence the name Pelletron accelerator. In a usual Van De Graff generator, the charges are carried out with the help of a belt instead of chains as in the present case. The available different ion sources are as

follows:

- (i) He ions for negative He ions
- (ii) Negative ions for gaseous elements
- (iii) Cesium - A sputter ion source for all elements.

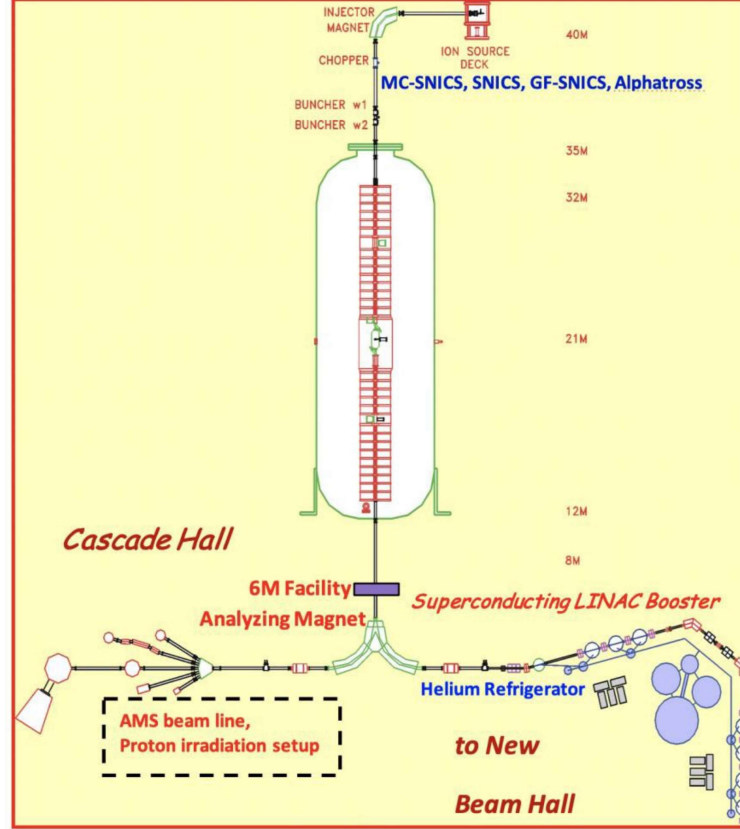


Figure 2.1: A collaborative Pelletron facility of BARC-TIFR.

Cesium sputter ion source which is a multi cathode negative ion source has been successfully employed [5,6]. The generated negative ions accelerated in the horizontal section at about 150-250 keV of energy and then these ions are allowed to be bent 90° through the magnets, and inserted into the vertical accelerating column. They are passing from a small volume of gas or a thin carbon foil, known as a stripper where they lose electrons and gain a high positive charge of p units will be $(p+1)V$, where V is the terminal voltage. The sulphur hexafluoride (SF_6) gas is used for insulation between terminals of the accelerator tank. It is possible to accelerate the beam from

the proton to Uranium. Also, pulsed beam and fully striped beam up to Chlorine is possible to obtain for various applications. Figure 2.1 represents a diagram of the accelerator.

This BARC-TIFR accelerator is extensively utilized for the neutron and proton irradiation experiment for various energies. The generation of the neutrons was obtained via ${}^7\text{Li}(p, n)$ reaction of 7-20 MeV of proton beams delivered from the pelletron to perform the neutron irradiation. On the other hand, the 16 MeV of the proton beam was delivered for the proton irradiation experiment. The detail of neutron and proton irradiation set up in the §2.2.1 & §2.2.2, respectively

2.2.1 Neutron Irradiation

The neutrons and neutron flux monitor are required for the experiment. The six meter of elevation level (above analyzing magnet) of the PLF facility has been adopted for the irradiation experiment. A pictorial form of the 6M irradiation port is presented in Fig. 2.2.



Figure 2.2: Pictorial view of 6M irradiation port.

For neutron generation, the ${}^7\text{Li}(p, n)$ reaction was utilized. The ${}^{nat}\text{Li}$ metal foil

was used for this purpose. The dimension of the target should be specific. If the target is thick then proton energy will degrade as it passes through the target and the definition of the incident beam will be altered. Also, the low energy radionuclide like evaporation residues will stop inside the target. Therefore, a thin backing self-supportive target is required. The rolling technique facility of the target preparation lab at TIFR was utilized to prepare targets. The specific assembly was designed to handle the Lithium target due to it being flammable when exposed to air [3]. The target foils used for the experiment have an area of approximately $1 \times 1 \text{ cm}^2$, to avoid area correction in the calculation of neutron flux. The targets were separately covered in thin Aluminium foil to prevent radioactive contamination. Further, ^{nat}Li metal foil of 3.4 mg/cm^2 thickness was implanted in the middle of the Tantalum (Ta) foils. The Ta foils were utilized in the radiation environment because Tantalum has a high ability to resist corrosion, good machinability, and lesser induced generation activity. The Ta foil placed in front of the target, facing the proton beam was of thickness 3.7 mg/cm^2 which is thin to prevent proton energy reduction. The proton energy degradation was estimated utilizing the SRIM [7] code. The Ta foil was kept behind the Li target is comparatively thick of order 4.12 mg/cm^2 to prevent the proton beam from hitting directly to the samples. The Ta foil stopped the proton beam which is isolated from the chamber and connected to an MHV for beam current measurement on Li target foil during the experiment. Simultaneously, the generated neutron passes and enters into the isolated zone where the samples were covered with the Aluminium foil and were kept 2.1 cm away from the stack of Ta-Li-Ta and zero degrees concerning the beam direction. We have tried to keep a steady current during the experiment. The samples were taken for γ ray counting to HPGe detector after the irradiation and sufficient cooling.

2.2.2 Proton Irradiation

The proton irradiation was performed using the stacked foil activation method at the BARC-TIFR pelletron. The targets and degraders of the appropriate thickness were used in the form of a stack. The Copper degrader is used for the energy degradation followed by the target foils. The degradation calculation was performed using

MCNP 6.2 code [8] as well as with SRIM code [7]. A constant current is utilized during the experiment. The proton flux was measured by the proton current. This assembly was placed inside 6 m of irradiation port shown in Fig. 2.2 for the proton beam irradiation. Then, these active targets were taken for γ ray counting to the HPGe detector.

2.3 Gamma ray spectrometry

It is an analytical method used to identify different radioactive isotopes of the sample. The activity detection of the irradiated samples was performed using offline γ ray spectroscopy. The gamma rays produced by the radioactive sources have different energies and intensities. The emission of gamma rays are detected and analysed utilizing the spectroscopy method. The delayed gamma rays coming from the activated samples were detected utilizing the HPGe detector in the form of the γ ray spectrum.

2.3.1 HPGe Detector

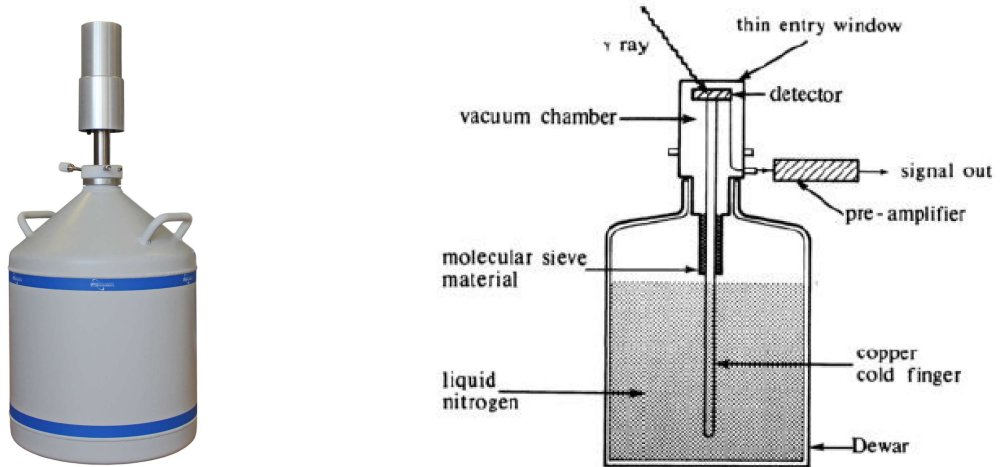


Figure 2.3: Schematic representation of HPGe detector.

The γ ray spectroscopy is utilized to measure the radioactive concentration of artificial and natural radionuclides using a high purity germanium detector (HPGe). The γ rays emitted because of the de-excitation of the radioactive nuclei can be detected using an HPGe detector having an excellent resolution and reasonable efficiency [9,10]. Figure 2.3 represents schematics of the HPGe detector.

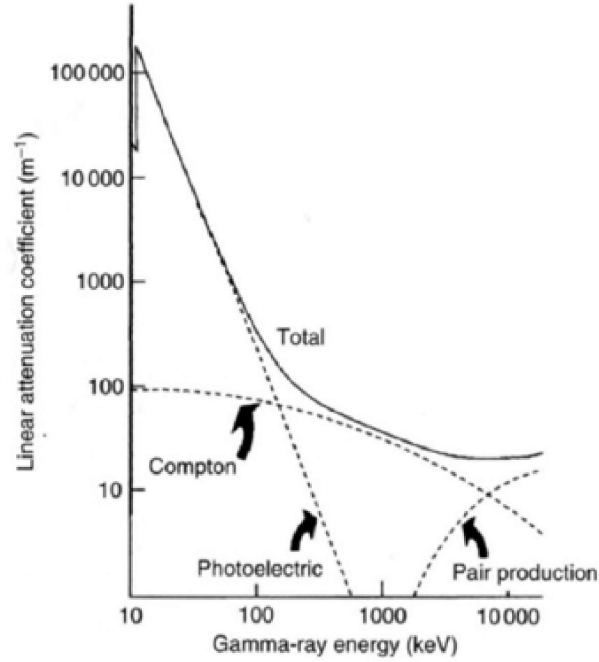


Figure 2.4: The linear attenuation coefficient of Ge and its basic parts [13].

HPGe falls into the category of semiconductor detector and due to low impurity concentration of about 10^{10} atoms/cm³ in Ge crystal, it is capable of achieving relatively thick depletion regions. The detector needs to be cooled for the reduction of the thermal charge carriers generation to an admissible level otherwise it will destroy the energy resolution of the detector. The detector can be cooled down using a very low temperature (-196°C or 77 K) of liquid nitrogen. The electron-hole pair is produced when photons enter the Germanium crystal by ionizing the atoms of the semiconductor. The number of generated electron-hole pairs is directly proportional to the energy of the radiation to the semiconductor. Therefore, several electrons are transferred from the valence band to the conduction band, and an equal number of holes are

created in the valence band. Germanium can absorb high energy photons up to a few MeV as it can have depleted to the sensitive thickness of centimeters. The electrons and holes (charge carriers) travel to the electrodes, where they result in a voltage pulse that carries the information of incident radiation and can be measured in a circuit [11,12]. The γ rays interact with the material via three processes, photoelectric effect, Compton scattering, and pair production. The photoelectric interactions are important at low energies, pair production at high energies and Compton scattering is the crucial interaction in the mid-energy range. The photoelectric interaction is the main process for detection purposes, in which a complete range of photons has been absorbed by electrons. The relative magnitudes due to these effects are presented in Fig. 2.4.

2.3.2 Resolution and Calibration of detector

Resolution is the ability of the detector to accurately calculate the incoming γ radiation energy. It can be defined as the Full Width at Half Maximum (FWHM) divided by the centroid (E) of a γ peak. Further, FWHM can be defined as,

$$\text{FWHM} = 2\sigma(2\ln 2)^{1/2} = 2.355 \sigma$$

where, σ is a standard deviation.

The (%) resolution (R) at a given energy E can be defined as,

$$R = (\text{FWHM} / E) * 100 \%$$

The smaller the R, the better the energy resolution of the detector.

The resolution of the detector expressed by FWHM of 1.8 keV at 1332.5 keV γ -line of ^{60}Co . As the HPGe detector has an energy band gap of 0.67 eV at 300 K, it produces leakage current at room temperature and is operated at 77 K.

A suitable energy calibration was carried out for the identification of γ ray emission energy. The multi gamma ray point-like source ^{152}Eu having a half-life of $\tau_{1/2} = 13.517$ y was used for calibration. The source may decay into various well resolved γ rays with

considerable intensity having a wide energy region from 121.78 to 1408.01 keV [14] is listed in Table 2.1 and the characteristic γ ray spectra of ^{152}Eu source is presented in Fig. 2.5.

Table 2.1: The γ ray energies of ^{152}Eu used for HPGe detector calibration.

γ Energy (keV)	γ intensity (%)
121.7817	28.53
244.6974	7.55
344.2785	26.59
411.1165	2.237
443.965	2.821
778.904	12.94
964.079	14.6
1112.076	13.67
1408.013	20.87

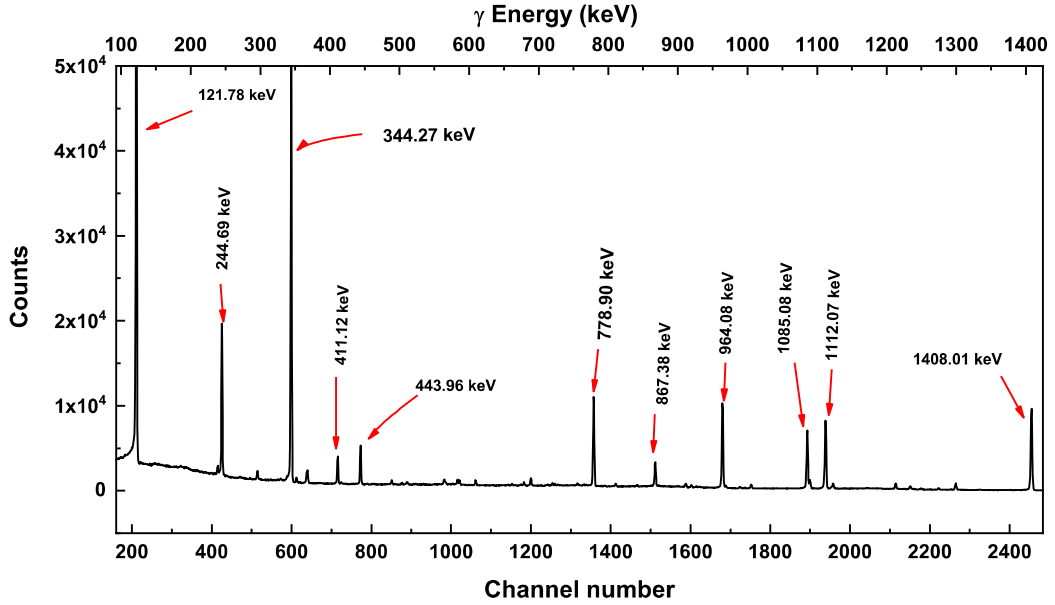


Figure 2.5: The γ -ray spectrum obtained from a calibrated ^{152}Eu reference source.

2.3.3 Detector efficiency

The efficiency (ϵ) is defined as the ratio of γ counts in a photo peak to the number of emitted gammas from the source. As efficiency varies with the γ -energy (E_γ), the efficiency calibration is done using the same ^{152}Eu source. The efficiency depends on the detector, the gamma energy, and the geometry of measurement. One can calculate efficiency utilizing the formula presented below [15],

$$\epsilon = \frac{C}{I_\gamma A_0 e^{-\lambda t}} \quad (2.1)$$

Where, C = counts of γ ray peak, a = γ abundance, A_0 = activity of source at the source calibration, A = activity of source at the counting time, λ = decay constant, t = time elapsed between the detector calibration and source calibration.

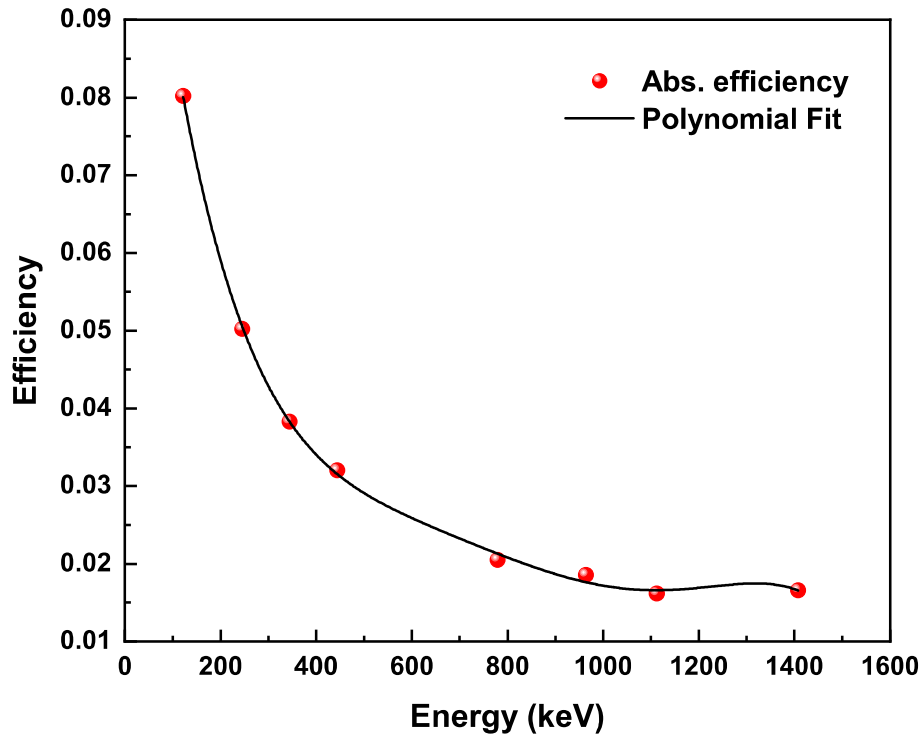


Figure 2.6: Measured efficiency for the HPGe detector.

The auxiliary quantities i.e. A_0 , I_γ , and λ were known before the experiment and counts are only the measured quantity collected from γ ray spectra. The efficiency was calculated using the same Eu source and presented in Fig. 2.6.

Bibliography

- [1] Robert W. Hamm and Marianne E. Hamm (R & M Technical Enterprises, California, USA), World Scientific, ISBN-13978-981-4307-04-8.
- [2] BARC-TIFR Pelletron facility, Mumbai, Official website: <https://www.tifr.res.in/~pell/pelletron/index.php>.
- [3] A. K. Gupta *et al.*, Proceedings of HLAT09, Venice, Italy.
- [4] R. P. Sharma, Nucl. Instrum. Methods Phys. Res. A **244**, 52 (1986).
- [5] Vandana Nanal and B. K. Nayak, Nucl. Phys. News Vol. **28** (4), (2018).
- [6] K. G. Prasad, Nucl. Instrum. Methods Phys. Res. B **40/41**, 916 (1989).
- [7] J. F. Ziegler: SRIM-2003. Nucl. Inst. Methods Phys. Res. B **1027**, 219-220 (2004), Available at <http://www.srim.org/>.
- [8] MCNP Users Manual - Code Version 6.2, edited by C. J. Werner, Los Alamos National Laboratory Report No. LA-UR-17-29981, 2017 (unpublished).
- [9] K. Szymanńska *et al.*, Nucl. Instrum. Methods Phys. Res. A **592**, 486-492 (2008).
- [10] I. Hossain *et al.*, Sci. Res. Essays **7**(1), 86-89 (2012).
- [11] Glenn F Knoll, Radiation Detection and Measurement 4th Edition, Wiley, 8/2010. ISBN-13:978-0470131480
- [12] A. J. Tavendale and G. T. Ewan, Nucl. Instrum. Methods Phys. Res. **25**, 185-187 (1964).

- [13] G. R. Gilmore. “Practical Gamma-ray Spectrometry”, Second Edition, Published by Wiley-VCH Verlag, Weinheim, Germany, 2008.
- [14] Nudat 2.7 β 2011, National Nuclear Data Center, Brookhaven National Laboratory, <https://www.nndc.bnl.gov/>
- [15] B. S. Shivashankar *et al.*, Nucl. Sci. and Eng. **179**, 423-433 (2017).